5626 *Inorg. Chem.* **2009**, *48*, 5626–5635
DOI: 10.1021/ic900600z

Inorganic Chemistry
Article

New Porphyrins Bearing Pyridyl Peripheral Groups Linked by Secondary or Tertiary Sulfonamide Groups: Synthesis and Structural Characterization

Janet Manono, Patricia A. Marzilli, Frank R. Fronczek, and Luigi G. Marzilli*

Department of Chemistry, Louisiana State University, Baton Rouge, Louisiana 70803

Received March 28, 2009

New pyridyl *meso*-tetraarylporphyrins (TArP, Ar = -C_6H_4-) of the general formula, T($R^1R^2NSO_2$Ar)P (R^1 = *N*-py-*n*-CH_2 (*n* = 2 or 4) and R^2 = CH_3), have been synthesized by the versatile approach of utilizing *meso*-tetra(4-chlorosulfonylphenyl)porphyrin. After characterization by mass spectrometry and by visible absorption and ^{1}H NMR spectroscopy, the porphyrins were converted to various metalloderivatives, including Cu(II) and Zn(II). Treatment of T(*N*-py-4-$CH_2(CH_3)NSO_2$Ar)P (**5**) or TpyP(4) (*meso*-tetra(4-pyridyl)porphyrin) with $CH_3Co(DH)_2H_2O$ (DH = monoanion of dimethylglyoxime) afforded $[CH_3Co(DH)_2]_4$T(*N*-py-4-$CH_2(CH_3)NSO_2$Ar)P (**6**) and $[CH_3Co(DH)_2]_4$TpyP(4) (**7**). Typically, basic pyridines shift the axial methyl ^{1}H NMR signal of $CH_3Co(DH)_2$L upfield but leave the equatorial methyl signal unshifted. However, both signals for $[CH_3Co(DH)_2]_4$TpyP(4) are ~0.2 ppm more downfield than normal, suggesting perhaps an extremely non-basic pyridyl group. However, TpyP(4) forms $CH_3Co(DH)_2$py adducts with binding ability comparable to that of other pyridine ligands with normal basicity and to that of T(*N*-py-4-$CH_2(CH_3)NSO_2$Ar)P. Consequently, in **7** the deshielding of the methyl signals, even the axial Co−CH_3 signal, is attributed to anisotropy of the porphyrin core. The methyl signals for $[CH_3Co(DH)_2]_4$T(*N*-py-4-$CH_2(CH_3)NSO_2$Ar)P (**6**) have normal shifts. The absence of an anisotropic effect is attributable to the large distance of the $CH_3Co(DH)_2$ moieties from the porphyrin core caused by the intervening linker in **6**. Indeed, the separation led to only a slightly reduced (25%) fluorescence emission of **6** compared to **5**, whereas that of **7** is considerably reduced (90%) compared to TpyP(4). The X-ray structures of **5**, its Cu(II) complex, and $[CH_3Co(DH)_2]_4$TpyP(4) (**7**) (all of which have C_i symmetry) support the spectroscopy. For example, the Co−N_{ax} bond lengths of $[CH_3Co(DH)_2]_4$TpyP(4) (2.055(4) and 2.079(4) Å) are comparable to that of $CH_3Co(DH)_2$py (2.068(3) Å), consistent with the normal coordinating ability of TpyP(4). In an accompanying study, the new pyridylporphyrins have been converted to DNA-binding, water-soluble cationic porphyrins.

Introduction

The special characteristics of porphyrins have led to numerous studies and applications both by nature and by mankind.[1−3] Pyridylporphyrins (PyPs) in which the pyridine ring is directly attached to the porphyrin core have been used in supramolecular systems, usually with metal centers providing the linking group.[4−6] A number of complexes with different coordination numbers involving ruthenium, rhenium, and platinum have been coordinated symmetrically to N atoms of the peripheral pyridyl groups of *meso*-tetrapyridylporphyrins (TpyPs).[5,7−10] Most studies have involved the *meso*-tetra(4-pyridyl)porphyrin (TpyP(4)) isomer, Chart 1. It has been shown that coordination of the different metal fragments to N atoms of the peripheral pyridyl groups not only solubilizes the porphyrin but also introduces useful functionalities into the system.[6] For example, Alessio and co-workers recently reported adducts between a TpyP(4) pyridyl group and either one or four Re(I) bipyridine tricarbonyl units, and they have compared their photophysical properties to those of the parent TpyP(4).[11]

*To whom correspondence should be addressed. E-mail: lmarzil@lsu.edu.

(1) *The Porphyrin Handbook*; Kadish, K. M., Smith, K. M., Guilard, R., Eds.; Academic Press: New York, 2000; Vol. 1−10.
(2) Kumar, R. K.; Goldberg, I. *Chem. Commun. (Cambridge, U. K.)* **1998**, 1435–1436.
(3) Liu, J.; Huang, J.-W.; Fu, B.; Zhao, P.; Yu, H.-C.; Ji, L.-N. *Spectrochim. Acta, Part A* **2007**, *67*, 391–394.
(4) Alessio, E.; Iengo, E.; Marzilli, L. G. *Supramol. Chem.* **2002**, *14*, 103–120.
(5) Alessio, E.; Macchi, M.; Heath, S. L.; Marzilli, L. G. *Inorg. Chem.* **1997**, *36*, 5614–5623.
(6) Gianferrara, T.; Serli, B.; Zangrando, E.; Iengo, E.; Alessio, E. *New J. Chem.* **2005**, *29*, 895–903.
(7) Anson, F. C.; Shi, C. N.; Steiger, B. *Acc. Chem. Res.* **1997**, *30*, 437–444.
(8) Castriciano, M.; Romeo, A.; Romeo, R.; Scolaro, L. M. *Eur. J. Inorg. Chem.* **2002**, 531–534.
(9) Araki, K.; Silva, C. A.; Toma, H. E.; Catalani, L. H.; Medeiros, M. H. G.; Di Mascio, P. *J. Inorg. Biochem.* **2000**, *78*, 269–273.
(10) Kon, H.; Tsuge, K.; Imamura, T.; Sasaki, Y.; Ishizaka, S.; Kitamura, N. *Inorg. Chem.* **2006**, *45*, 6875–6883.
(11) Ghirotti, M.; Chiorboli, C.; Indelli, M. T.; Scandola, F.; Casanova, M.; Iengo, E.; Alessio, E. *Inorg. Chim. Acta* **2007**, *360*, 1121–1130.

Published on Web 06/11/2009

Chart 1

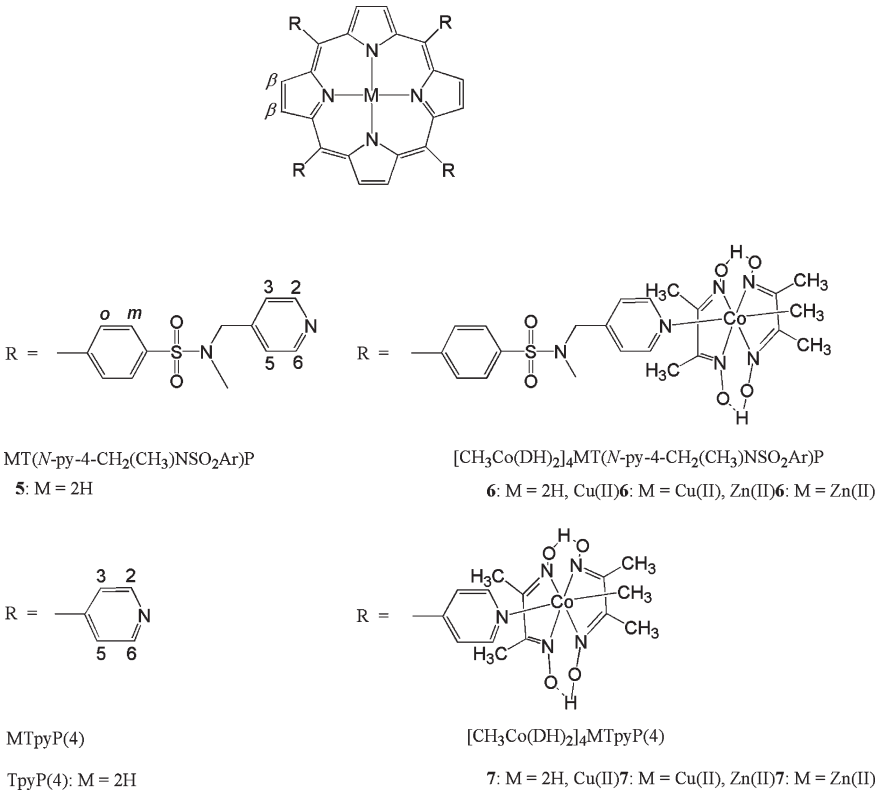

A second type of application for PyPs, such as TpyP(4), is to convert them into water-soluble *N*-alkylpyridinium derivatives. These compounds have been shown to possess interesting biomedical properties such as antiviral activity, anticancer activity, and so on, and to interact with DNA by a variety of binding modes.[12−16] In many cases, metals bound to the center of the porphyrin influence the DNA binding mode.[17−21] Coordination of areneruthenium(II) compounds (e.g., $[Ru(\eta^6\text{-}C_6H_5CH_3)(\mu\text{-}Cl)Cl]_2$) to the pyridyl groups of TpyP(4) to form $[Ru(\eta^6\text{-}C_6H_5CH_3)Cl_2]_4$TpyP(4) has been studied with the aim of combining the photodynamic action of the porphyrin with the cytotoxicity of the areneruthenium complexes.[22] These PyPs are generally relatively rigid, a property that may be helpful in constructing supramolecular systems,[23,24] but it would be interesting to examine less rigid systems. However, our interest in less rigid systems was mainly motivated by our program to study DNA binding of cationic porphyrins, particularly after the pyridines are converted to *N*-alkyl pyridinium groups.[25] As a first step in this direction, we wanted to overcome some of the problems in constructing suitable porphyrins, chiefly the low-yield syntheses that hamper porphyrin chemistry and the poor solubility of such PyPs as TpyP(4). PyPs reported here were prepared from the simple *meso*-tetraphenylporphyrin (TPP). TPP can be modified by connecting to it different peripheral substituents, changing the central metal, or expanding the size of the macrocycle. In this initial report, we employ a very useful strategy to meet our goals of finding a versatile synthetic approach to preparing soluble PyPs containing sulfonamide groups of the general formula, MT($R^1R^2NSO_2Ar$)P (Scheme 1 and Chart 1). The new pyridyl *meso*-tetraarylporphyrins (TArP, Ar = -C_6H_4-) of the general formula, T($R^1R^2NSO_2Ar$)P (R^1 = *N*-py-*n*-CH_2 (*n* = 2 or 4) and R^2 = H or alkyl) are synthesized by the versatile approach of utilizing *meso*-tetra(4-chlorosulfonylphenyl) porphyrin (**1**, Scheme 1). However, we found previously that intractable products are obtained when R^1 = H (such as **2** and **3** in Scheme 1). Here we report new more tractable pyridylporphyrins, T($R^1R^2NSO_2Ar$)P (R^1 = *N*-py-*n*-CH_2 (*n* = 2 or 4) and R^2 = CH_3, Scheme 1 and Chart 1).

Using ^{1}H NMR, visible absorption, and fluorescence spectroscopic techniques, we have examined the effect of coordination of the methylcobaloxime ($CH_3Co(DH)_2$) moiety (DH = the monoanion of dimethylglyoxime) to the *N*-pyridyl group of the newly synthesized porphyrin, T(*N*-py-4-$CH_2(CH_3)NSO_2Ar$)P. Good solubility allows facile addition

(12) Carvlin, M. J.; Fiel, R. J. *Nucleic Acids Res*. **1983**, *11*, 6121–6139.
(13) Fiel, R. J. *J. Biomol. Struct. Dyn*. **1989**, *6*, 1259–1275.
(14) Fiel, R. J.; Howard, J. C.; Mark, E. H.; Dattagupta, N. *Nucleic Acids Res*. **1979**, *6*, 3093–3118.
(15) Fiel, R. J.; Munson, B. R. *Nucleic Acids Res*. **1980**, *8*, 2835–2842.
(16) Marzilli, L. G. *New J. Chem*. **1990**, *14*, 409–420.
(17) Banville, D. L.; Marzilli, L. G.; Strickland, J. A.; Wilson, W. D. *Biopolymers* **1986**, *25*, 1837–1858.
(18) Pasternack, R. F.; Gibbs, E. J.; Villafranca, J. J. *Biochemistry* **1983**, *22*, 5409–5417.
(19) Strickland, J. A.; Banville, D. L.; Wilson, W. D.; Marzilli, L. G. *Inorg. Chem*. **1987**, *26*, 3398–3406.
(20) Ward, B.; Skorobogaty, A.; Dabrowiak, J. C. *Biochemistry* **1986**, *25*, 7827–7833.
(21) Gibbs, E. J.; Tinoco, I.; Maestre, M. F.; Ellinas, P. A.; Pasternack, R. F. *Biochem. Biophys. Res. Commun*. **1988**, *157*, 350–358.
(22) Schmitt, F.; Govindaswamy, P.; Süss-Fink, G.; Ang, W.; Dyson, P. J.; Juillerat-Jeanneret, L.; Therrien, B. *J. Med. Chem*. **2008**, *51*, 1811–1816.
(23) *Comprehensive Supramolecular Chemistry*; Atwood, L. J., Davies, D. E. J., Mac Nicol, D. D., Vogtle, F., Reinhoudt, N. D., Eds.; Pergamon Press: Oxford, 1996.
(24) Balzani, V.; Scandola, F. *Supramolecular Photochemistry*; Horwood: Chichester, U.K., 1991.
(25) Manono, J.; Marzilli, P. A.; Marzilli, L. G. *Inorg. Chem*. **2009**, DOI: 10.1021/ic900385y.

Scheme 1. Synthetic Scheme and Some Porphyrins Mentioned in This Work

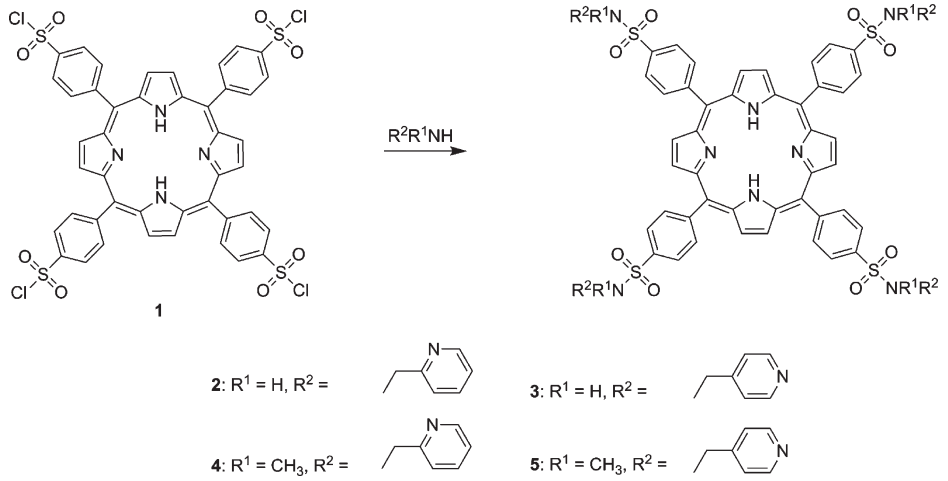

of the metal to either the inner core of the porphyrin or to a peripheral pyridyl group. Furthermore, we report a method of making poorly soluble porphyrins (e.g., TpyP(4)) more soluble by using the ($CH_3Co(DH)_2$) moiety as a dissociable metal-protecting group. Organocobaloximes ($RCo(DH)_2L$), in which L is an N-donor ligand such as pyridine, have been used extensively to understand the fundamental chemistry related to the organocobalt B_{12} coenzymes.[26−32] Organocobaloximes undergo exchange of the trans axial ligand relatively rapidly, so that solutions normally reach equilibrium before NMR spectra can be recorded.[26] Methylcobaloximes have well-understood NMR properties because axial ligand exchange is slow on the NMR time scale. In this work we exploit these favorable properties to explore the new porphyrins we have prepared.

Experimental Section

Starting Materials. 4-Cyanopyridine (4-CNpy), pyridine (py), 3,5-lutidine (3,5-lut), 4-dimethylaminopyridine (4-Me_2-Npy), *n*-pyridylcarboxaldehyde (*n* = 2 or 4), methylamine (CH_3NH_2), *meso*-tetra(4-pyridyl)porphyrin (TpyP(4)), and all solvents were obtained from Sigma-Aldrich. 5,10,15,20-tetra-(4-chlorosulfonylphenyl)porphyrin ($TClSO_2PP$ (**1**), Scheme 1) was synthesized by a known method, and the ^{1}H NMR chemical shifts in $CDCl_3$ matched the reported values.[33] $CH_3Co(DH)_2$-H_2O was prepared as previously reported.[31]

Instrumentation. All ^{1}H NMR spectra were recorded on a 400 MHz Bruker NMR spectrometer. Peak positions are relative to TMS or solvent residual peak, with TMS as reference. Visible absorption spectra were recorded with a Cary 3 spectrophotometer. Excitation and fluorescence spectra of 5.0 μM porphyrin solutions (CH_2Cl_2) were recorded on a Fluorolog-3 spectrofluorimeter (Horiba Jobin Yvon) at room temperature.

X-ray Data Collection and Structure Determination. All single crystals suitable for X-ray crystallography were obtained by slow diffusion of methanol into dichloromethane solution. Single crystals were placed in a cooled nitrogen gas stream at 90 K on a Nonius Kappa CCD diffractometer fitted with an Oxford Cryostream cooler with graphite-monochromated Mo Kα (λ = 0.71073 Å) radiation. Data reduction included absorption corrections by the multiscan method, with HKL SCALEPACK.[34] All X-ray structures were determined by direct methods and difference Fourier techniques and refined by full-matrix least-squares, using SHELXL97.[35] All non-hydrogen atoms were refined anisotropically. All hydrogen atoms were visible in difference maps, but were placed in idealized positions, except for those of the OH groups in **7**, for which coordinates were refined. A torsional parameter was refined for each methyl group.

Synthesis of T(*N*-py-*n*-$CH_2(CH_3)NSO_2Ar$)P Porphyrins (*n* = 2 or 4). Porphyrins **4** and **5** (below) were synthesized from secondary amines, prepared by a slight modification of a published procedure.[36] A solution of 1.0 g (9.34 mmol) of *n*-pyridylcarboxaldehyde (*n* = 2 or 4) in water (5 mL) was saturated with methylamine gas until the solution was cloudy. The resulting solution was stirred at RT for 2 h. Solvent removal under vacuum left a pale yellow oil of the Schiff base (~1.0 g); Schiff base formation was confirmed by a characteristic ^{1}H NMR imine signal (*N*-(4-pyridylmethylene)methylamine at 8.16 ppm, *N*-(2-pyridylmethylene)methylamine at 8.35 ppm). The yellow oil (9.34 mmol) was dissolved in 10 mL of methanol, 0.472 g of $NaBH_4$ was added, and the reaction mixture then left stirring at RT for 30 min. The solvent was evaporated under vacuum; the residue was dissolved in water (10 mL) and extracted into CH_2Cl_2 (3 × 10 mL). The organic phase was dried over anhydrous Na_2SO_4, and the solvent evaporated under vacuum to yield pale yellow oils that were characterized by ^{1}H NMR spectroscopy. These oils were used to synthesize porphyrins **4** and **5** as follows: a solution of **1** (0.2 g, 0.198 mmol) in CH_2Cl_2 (20 mL) was treated with 0.11 g (0.89 mmol) of *N*-methyl-*N*-(*n*-pyridylmethyl)amine (*n* = 2 or 4) in CH_2Cl_2 (5 mL). The reaction mixture was stirred at RT overnight, and the precipitate that formed was removed by filtration. The filtrate was washed with water (3 × 15 mL), dried over

(26) Bresciani-Pahor, N.; Forcolin, M.; Marzilli, L. G.; Randaccio, L.; Summers, M. F.; Toscano, P. J. *Coord. Chem. Rev.* **1985**, *63*, 1–125.
(27) Marzilli, L. G.; Summers, M. F.; Bresciani-Pahor, N.; Zangrando, E.; Charland, J. P.; Randaccio, L. *J. Am. Chem. Soc.* **1985**, *107*, 6880–6888.
(28) Parker, W. O.; Zangrando, E.; Bresciani-Pahor, N.; Randaccio, L.; Marzilli, L. G. *Inorg. Chem.* **1986**, *25*, 3489–3497.
(29) Siega, P.; Randaccio, L.; Marzilli, P. A.; Marzilli, L. G. *Inorg. Chem.* **2006**, *45*, 3359–3368.
(30) Summers, M. F.; Toscano, P. J.; Bresciani-Pahor, N.; Nardin, G.; Randaccio, L.; Marzilli, L. G. *J. Am. Chem. Soc.* **1983**, *105*, 6259–6263.
(31) Toscano, P. J.; Chiang, C. C.; Kistenmacher, T. J.; Marzilli, L. G. *Inorg. Chem.* **1981**, *20*, 1513–1519.
(32) Toscano, P. J.; Marzilli, L. G. *Prog. Inorg. Chem.* **1984**, *31*, 105–204.
(33) Gonsalves, A. M. R.; Johnstone, R. A. W.; Pereira, M. M.; de SantAna, A. M. P.; Serra, A. C.; Sobral, A. J. F. N.; Stocks, P. A. *Heterocycles* **1996**, *43*, 829–838.
(34) Otwinowski, Z.; Minor, W. *Macromolecular Crystallography, part A*; New York Academic Press: New York, 1997; Vol. 276.
(35) Sheldrick, G. M. *SHELX-97, Program for Crystal Structure Solution and Refinement*; University of Göttingen: Göttingen, Germany, 1997.
(36) Tanaka, K.; Shiraishi, R. *Green Chem.* **2000**, *2*, 272–273.

Table 1. Characteristic Absorption and Emission Maxima of Methylcobaloxime−Porphyrin Adducts and of the Porphyrin Models in CH_2Cl_2

	absorption (λ_{max}/nm)		emission	
compound	Soret band	Q bands	λ_{em} (nm)[a]	
T(*N*-py-4-$CH_2(CH_3)NSO_2Ar$)P (**5**)	420	514, 548, 589, 644	650	714
Cu(II)**5**	416	540		
Zn(II)**5**	424	550, 596	603	649
$[CH_3Co(DH)_2]_4$ Por**5** (**6**)	420	514, 548, 589, 644	650	714
Cu(II)**6**	416	540		
Zn(II)**6**	424	550, 596	599	648
TpyP(4)	416	510, 544, 587, 642	649	712
Cu(II)TpyP(4)	418	538		
Zn(II)TpyP(4)	424	550, 596	602	652
$[CH_3Co(DH)_2]_4$ TpyP(4) (**7**)	422	515, 550, 590, 646	652	714
Cu(II)**7**	418	540		
Zn(II)**7**	424	551, 594	603	646

[a] λ_{exc} = 420 nm.

anhydrous Na_2SO_4, and the solvent removed under vacuum. The residue was recrystallized from CH_2Cl_2/methanol.

T(*N*-py-2-$CH_2(CH_3)NSO_2Ar$)P (4). The general method described above, starting with 2-pyridylcarboxaldehyde (1 g, 9.34 mmol) and CH_3NH_2, yielded *N*-methyl-*N*-(2-pyridylmethyl) amine as a pale yellow oil (0.89 g, 76% yield). ^{1}H NMR (ppm) in $CDCl_3$: 8.53 (1H, d, ArH), 7.66 (1H, t, ArH), 7.28 (1H, d, ArH), 7.16 (1H, s, ArH), 3.83 (2H, s, CH_2), 2.50 (3H, s, CH_3).1.86 (1H, br, NH). GC-MS(*m*/*z*): M^+ = 123.2. Calcd for M^+ 123.17. Treatment of **1** (0.2 g, 0.198 mmol) with *N*-methyl-*N*-(2-pyridylmethyl)amine (0.11 g, 0.89 mmol) as described above afforded porphyrin **4** as a purple powder (0.16 g, 59% yield). ^{1}H NMR (ppm) in DMSO-d_6: 8.90 (8H, s, βH), 8.59 (4H, d, H2), 8.47 (8H, d, *m*H), 8.25 (8H, d, *o*H), 7.90 (4H, m, H3), 7.56 (4H, d, H5), 7.39 (4H, m, H4), 4.60 (8H, s, CH_2), 2.99 (12H, CH_3), −2.94 (2H, br, NH). ESI-MS(*m*/*z*): $[M + H]^+$ = 1351.4077, $[M + 2H]^{+2}$ = 676.2076, $[M + 3H]^{+3}$ = 451.1437. Calcd for $[M + H]^+$ = 1351.3775, $[M + 2H]^{+2}$ = 676.1926, $[M + 3H]^{+3}$ = 451.1310.

T(*N*-py-4-$CH_2(CH_3)NSO_2Ar$)P (5). The general method described above, starting with 4-pyridylcarboxaldehyde (1 g, 9.34 mmol) and CH_3NH_2, yielded *N*-methyl-*N*-(4-pyridylmethyl) amine as a pale yellow oil (0.94 g, 83% yield). The ^{1}H NMR spectrum in $CDCl_3$ matches that reported in the literature.[37] ^{1}H NMR (ppm) in $CDCl_3$: 8.53 (2H, d, ArH), 7.24 (2H, d, ArH), 3.77 (2H, s, CH_2), 2.46 (3H, s, CH_3), 1.98 (1H, br, NH). GC-MS (*m*/*z*): M^+ = 123.0. Calcd for M^+ 123.17. Treatment of **1** (0.2 g, 0.198 mmol) with *N*-methyl-*N*-(4-pyridylmethyl)amine (0.11 g, 0.89 mmol) as described above afforded porphyrin **5** as a purple powder (0.15 g, 55% yield). ^{1}H NMR (ppm) in DMSO-d_6: 8.92 (8H, s, βH), 8.65 (8H, d, H2,6), 8.51 (8H, d, *m*H), 8.30 (8H, d, *o*H), 7.46 (8H, d, H3,5), 4.54 (8H, s, CH_2), 2.93 (12H, s, CH_3), −2.92 (2H, br, NH). ESI-MS(*m*/*z*): $[M + H]^+$ = 1351.4107, $[M + 2H]^{+2}$ = 676.2096, $[M + 3H]^{+3}$ = 451.1451. Calcd for $[M+H]^+$ = 1351.3775, $[M + 2H]^{+2}$ = 676.1926, $[M+3H]^{+3}$ = 451.1310.

Cu(II)T(*N*-py-4-$CH_2(CH_3)NSO_2Ar$)P (Cu(II)5). A solution of **5** (50 mg, 0.037 mmol) in CH_2Cl_2 (10 mL) was treated with copper(II) acetate (6.4 mg, 0.037 mmol) in methanol (5 mL). The solution was left stirring at RT for about 1 h. Completion of the reaction was indicated by the collapse of the four Q bands of the free base to one Q-band (Table 1). The reaction mixture was reduced in volume to about 1 mL, and acetone was added to precipitate Cu(II)**5** as a red powder (48 mg, 92% yield). ^{1}H NMR (ppm) in $CDCl_3$, see Chart 1 for labeling: 8.74 (8H, br, H2,6), 8.05 (8H, br *m*H), 7.49 (8H, d, H3,5), 4.46 (8H, br, CH_2), 2.92 (12H, br, CH_3).

Zn(II)T(*N*-py-4-$CH_2(CH_3)NSO_2Ar$)P (Zn(II)5). A solution of **5** (50 mg, 0.037 mmol) in CH_2Cl_2 (10 mL) was treated with zinc(II) acetate (40 mg, 0.19 mmol) in methanol (2 mL). The solution was left stirring at RT for 2 h, after which an aliquot of the reaction mixture was analyzed by using visible spectroscopy. The metal insertion was complete, as indicated by the collapse of the four Q bands to two Q bands (Table 1). After the CH_2Cl_2 was removed by rotary evaporation, the purple precipitate that formed was collected on a filter and washed with methanol to remove the excess of zinc acetate and air-dried to afford Zn(II)**5** (30 mg, 58% yield). ^{1}H NMR (ppm) in DMSO-d_6, see Chart 1 for labeling: 8.85 (8H, s, βH), 8.64 (8H, d, H2,6), 8.46 (8H, d, *m*H), 8.28 (8H, d, *o*H), 7.46 (8H, d, H3,5), 4.55 (8H, d, CH_2), 2.93 (12H, s, CH_3).

Synthesis of ($[CH_3Co(DH)_2]$)$_4$T(*N*-py-4-$CH_2(CH_3)NSO_2Ar$)P (6). $CH_3Co(DH)_2H_2O$ (95 mg, 0.30 mmol) was added to a solution of **5** (0.1 g, 0.074 mmol) in CH_2Cl_2 (20 mL) and stirred until a clear solution resulted (∼5 min). The solution was filtered and treated with 5 mL of ethyl acetate. After partial evaporation of the solution, a brownish precipitate was collected on a filter, washed with diethyl ether, and vacuum-dried to afford **6** (Chart 1) as a brown precipitate (0.17 g, 92% yield). ^{1}H NMR (ppm) in $CDCl_3$, see Chart 1 for labeling: 18.34 (8H, s, OH), 8.85 (8H, s, βH), 8.67 (8H, d, H2,6), 8.44 (8H, d, *m*H), 8.26 (8H, d, *o*H), 7.44 (8H, d, H3,5), 4.54 (8H, d, CH_2), 3.00 (12H, CH_3), 2.15 (48H, s, CH_3), 0.82 (12H, d, Co-CH_3), −2.79 (2H, br, NH).

$[CH_3Co(DH)_2]_4$Cu(II)T(*N*-py-4-$CH_2(CH_3)NSO_2Ar$)P (Cu(II)6). The general method described above with $CH_3Co(DH)_2H_2O$ (45 mg, 0.14 mmol) and Cu(II)**5** (50 mg, 0.035 mmol) afforded Cu(II)**6** (Chart 1) as a red precipitate (65 mg, 69% yield). ^{1}H NMR (ppm) in $CDCl_3$, see Chart 1 for labeling: 18.30, (8H, s, OH), 8.62 (8H, br, H2,6), 8.02 (8H, br *m*H), 7.38 (8H, d, H3,5), 4.44 (8H, d, CH_2), 2.90 (12H, CH_3), 2.14 (48H, s, CH_3), 0.81 (12H, d, Co-CH_3).

$[CH_3Co(DH)_2]_4$Zn(II)T(*N*-py-4-$CH_2(CH_3)NSO_2Ar$)P (Zn(II)6). The general method described above with $CH_3Co(DH)_2H_2O$ (45 mg, 0.14 mmol) and Zn(II)**5** (50 mg, 0.035 mmol) afforded Zn(II)**6** (Chart 1) as a purple precipitate (50 mg, 53% yield). ^{1}H NMR (ppm) in $CDCl_3$, see Chart 1 for labeling: 18.18 (8H, s, OH), 8.94 (8H, s, βH), 8.63 (8H, d, H2,6), 8.44 (8H, d, *m*H), 8.24 (8H, d, *o*H), 7.41 (8H, d, H3,5), 4.54 (8H, d, CH_2), 3.01 (12H, CH_3), 2.12 (48H, s, CH_3), 0.77 (12H, d, Co-CH_3).

$[CH_3Co(DH)_2]_4$TpyP(4) (7). $CH_3Co(DH)_2H_2O$ (0.21 g, 0.64 mmol) was added to a suspension of TpyP**(4)** (0.1 g, 0.16 mmol) in CH_2Cl_2 (10 mL). After stirring (∼5 min), the suspension became a solution, which was then filtered and 5 mL of ethyl acetate was added. After partial evaporation of the solution, a reddish precipitate was collected on a filter, washed with diethyl ether, and vacuum-dried to afford **7** (Chart 1, 0.28 g, 94% yield). ^{1}H NMR (ppm) in $CDCl_3$, see Chart 1 for labeling: 18.53 (8H, s, OH), 9.03 (8H, d, H2,6), 8.75 (8H, s, βH), 8.15 (8H, d, H3,5), 2.33 (48H, s, CH_3), 1.03 (12H, s, Co-CH_3), −3.04 (2H, br, NH).

$[CH_3Co(DH)_2]_4$Cu(II)TpyP(4) (Cu(II)7). A solution of **7** (50 mg, 0.027 mmol) in CH_2Cl_2 (10 mL) was treated with a methanol solution (5 mL) of Cu(II) acetate (8.2 mg, 0.041 mmol). The solution was stirred at RT for 2 h, then filtered and left standing at RT overnight. The precipitate that formed was collected on a filter and vacuum-dried, affording Cu(II)**7** (Chart 1) as a red precipitate (43 mg, 85%). ^{1}H NMR (ppm) in $CDCl_3$, see Chart 1 for labeling: 18.23 (8H, s, OH), 8.79 (8H, br, H2,6), 2.26 (48H, s, CH_3), 0.96 (12H, s, Co-CH_3).

$[CH_3Co(DH)_2]_4$Zn(II)TpyP(4) (Zn(II)7). Treatment of a solution of **7** (50 mg, 0.027 mmol) with a methanol solution (5 mL) of Zn(II) acetate (8.9 mg, 0.041 mmol) as described for Cu(II)**7** above afforded Zn(II)**7** (Chart 1) as a purple precipitate

(37) Varney, M. D.; Palmer, C. L.; Deal, J. G.; Webber, S.; Welsh, K. M.; Bartlett, C. A.; Morse, C. A.; Smith, W. W.; Janson, C. A. *J. Med. Chem.* **1995**, *38*, 1892–1903.

Table 2. Crystal Data and Structure Refinement for T(*N*-py-4-$CH_2(CH_3)$-NSO_2Ar)P (**5**), Cu(II)**5**, and $[CH_3Co(DH)_2]_4$TpyP(4) (**7**)

	5	Cu(II)**5**	**7**
formula	$C_{72}H_{62}N_{12}O_8S_4\cdot 4CH_3OH$	$C_{72}H_{60}CuN_{12}O_8S_4\cdot 4CH_3OH$	$C_{76}H_{94}Co_4N_{24}O_{16}\cdot 12CHCl_3$
fw	1479.74	1541.27	3267.89
color	red	orange	orange
cryst syst	monoclinic	monoclinic	triclinic
space group	$P2_1/c$	$P2_1/c$	$P\bar{1}$
		unit cell dimensions	
a (Å)	13.879(5)	13.530(4)	13.356(2)
b (Å)	12.776(4)	12.967(4)	13.893(2)
c (Å)	21.131(8)	21.020(7)	19.974(4)
α (deg)	90	90	72.830(9)
β (deg)	99.184(15),	97.227(14)	73.905(7)
γ (deg)	90	90	75.270(9)
V (Å^3)	3699(2)	3659(2)	3341.7(10)
Z	2	2	1
T (K)	90	90	90
ρ_{calc} (mg m^{-3})	1.329	1.399	1.624
abs coeff (mm^{-1})	0.20	0.48	1.27
$2\theta_{max}$ (deg)	46.0	46.0	46.0
R indices[a]	0.090	0.096	0.051
wR2 = $[I > 2\sigma(I)]$[b]	0.247	0.280	0.136
data/params	5081/471	5066/477	9107/795

[a] $R = \sum||F_o| - |F_c||/\sum|F_o|$. [b] $wR2 = [\sum[w(F_o^2 - F_c^2)^2]/\sum[w(F_o^2)^2]]^{1/2}$.

(39 mg, 77% yield). ^{1}H NMR (ppm) in $CDCl_3$, see Chart 1 for labeling: 18.42(8H, s, OH), 8.97 (8H, d, H2,6), 8.82 (8H, s, βH), 8.13 (8H, d, H3,5), 2.29 (48H, s, CH_3), 0.97 (12H, s, Co-CH_3).

Results and Discussion

Crystal Structures of T(*N*-py-4-$CH_2(CH_3)NSO_2Ar$)P (5) and Cu(II)T(*N*-py-4-$CH_2(CH_3)NSO_2Ar$)P (Cu(II)5). X-ray quality crystals of porphyrin **5** and its copper complex were obtained by slow diffusion of methanol into a dichloromethane solution of the respective compound. Crystal data and structural refinement details are summarized in Table 2. Oak Ridge Thermal Ellipsoid Plot (ORTEP) drawings of **5** and Cu(II)**5** are shown in Figure 1; **5** and Cu(II)**5** lie on inversion centers. The 24-atom core of **5** is nearly planar, having a mean deviation of 0.032 Å. The two distances (2.018 and 2.091 Å) from the centroid (C_t) of the pyrrole nitrogens to $N_{pyrrole}$ and $NH_{pyrrole}$, respectively, in **5** are comparable to the respective values of 2.026 and 2.099 Å for TPP.[38] The phenyl rings of **5** are almost perpendicular to the plane of the porphyrin, with dihedral angles of 84.9(2)° and 73.3 (2)°. Two of the pyridyl rings of **5** are almost parallel to the plane of the porphyrin, with a dihedral angle of 4.6(3)°, and the other two pyridyl rings form a dihedral angle of 36.1(3)° with the porphyrin plane.

The coordination about the copper atom of Cu(II)**5** is square planar (Figure 1). The two Cu−N distances are 2.001(5) and 2.002(6) Å, which are comparable to that for Cu(II)TPP (1.995(2) Å).[39] The phenyl rings of Cu(II)**5** are almost perpendicular to the plane of the porphyrin with dihedral angles of 83.5(3)° and 84.0(3)°. Two of the pyridyl rings of Cu(II)**5** are almost parallel to the plane of the porphyrin with a dihedral angle of 3.7(4)°, while the dihedral angle for the other two pyridyl rings is 31.2(5)°. The overlay of the porphyrin core of Cu(II)TPP and Cu (II)**5** gave an rms value of 0.014 Å. This good fit implies that having substituents at the periphery of the porphyrin does not affect the planarity of the core. Preliminary X-ray results also confirmed the synthesis of **4** (Supporting Information, Figure S1).

Crystal Structure of $[CH_3Co(DH)_2]_4$TpyP(4) (7). Crystals of porphyrin **7** were obtained by layering hexane in a chloroform solution of **7**. The crystals permitted the first X-ray structural determination of the TpyP(4) molecule with four $CH_3Co(DH)_2$ units, each bound to a pyridyl nitrogen (Table 2, Figure 2). In the crystal, the porphyrin has an inversion center. The planes of the pyridyl groups make dihedral angles of 78.1(2)° and 64.1(2)° with the plane of the porphyrin. The equatorial planes of the pseudo-octahedral methylcobaloxime units are nearly perpendicular to the plane of the porphyrin, with dihedral angles of 89.6(1)° and 81.4(1)°. The Co−N_{eq} bond distances range from 1.882(4)−1.892(5) Å (Supporting Information, Table S1), which is close to the range reported for $CH_3Co(DH)_2$py (1.877(2)−1.905(5) Å).[40] The Co−N(axial) distances of **7** are 2.055(4) and 2.079 (4) Å (Supporting Information, Table S1), in good agreement with the value reported for $CH_3Co(DH)_2$py (2.068 (3) Å).[40] The Co−CH_3 bond lengths of **7** (1.999(5) and 2.002(5) Å) are very close to the value reported for $CH_3Co(DH)_2$py (1.998(5) Å).[40]

Synthesis of the Porphyrins, Porphyrin-Cobaloxime Adducts, and Their Metal Complexes. Treatment of **1** ($TClSO_2PP$, Scheme 1) with primary amines such as 2- or 4-pyridylmethylamine generated porphyrins containing secondary sulfonamide groups (**2** and **3**).[41] Metalation of such porphyrins resulted in an insoluble material,[41] possibly because the metal coordinates to the sulfonamide group through both the sulfonyl oxygen and the deprotonated sulfonamide nitrogen.[42−44] The potential for secondary sulfonamides to coordinate to metals led us to investigate the synthesis of porphyrins containing only tertiary sulfonamide groups. The presence of an N-Me group in place of the dissociable NH group allowed us to prepare porphyrins (**4** and **5**) that are very soluble in organic solvents; these were characterized by mass spectrometry and ^{1}H NMR spectroscopy. Cu(II) and Zn(II) complexes of porphyrin **5** were also prepared.

Methylcobaloxime complexes ($CH_3Co(DH)_2L$) are generally synthesized from $CH_3Co(DH)_2H_2O$ by substitution of water in the presence of an excess of L in methanol solution[31] or in a CH_2Cl_2 suspension.[30] Addition in a 4:1 ratio of $CH_3Co(DH)_2H_2O$ to L (L = T(*N*-py-4-$CH_2(CH_3)NSO_2Ar$)P and TpyP(4)) in dichloromethane produced $[CH_3Co(DH)_2]_4$L adducts. The related metalloporphyrin adducts can be prepared by reaction of the metalloporphyrin with $CH_3Co(DH)_2H_2O$

(38) Fleischer, E. B.; Webb, L. E.; Miller, C. K. *J. Am. Chem. Soc.* **1964**, *86*, 2342–2347.
(39) He, H. S. *Acta Crystallogr., Sect. E: Struct. Rep. Online* **2007**, *63*, M976–M977.
(40) Bigotto, A.; Zangrando, E.; Randaccio, L. *J. Chem. Soc., Dalton Trans.* **1976**, 96–104.
(41) Manono, J.; PhD. Dissertation, Louisiana State University, 2009.
(42) Saladini, M.; Iacopino, D.; Menabue, L. *J. Inorg. Biochem.* **2000**, *78*, 355–361.
(43) Christoforou, A. M.; Fronczek, F. R.; Marzilli, P. A.; Marzilli, L. G. *Inorg. Chem.* **2007**, *46*, 6942–6949.
(44) Christoforou, A. M.; Marzilli, P. A.; Fronczek, F. R.; Marzilli, L. G. *Inorg. Chem.* **2007**, *46*, 11173–11182.

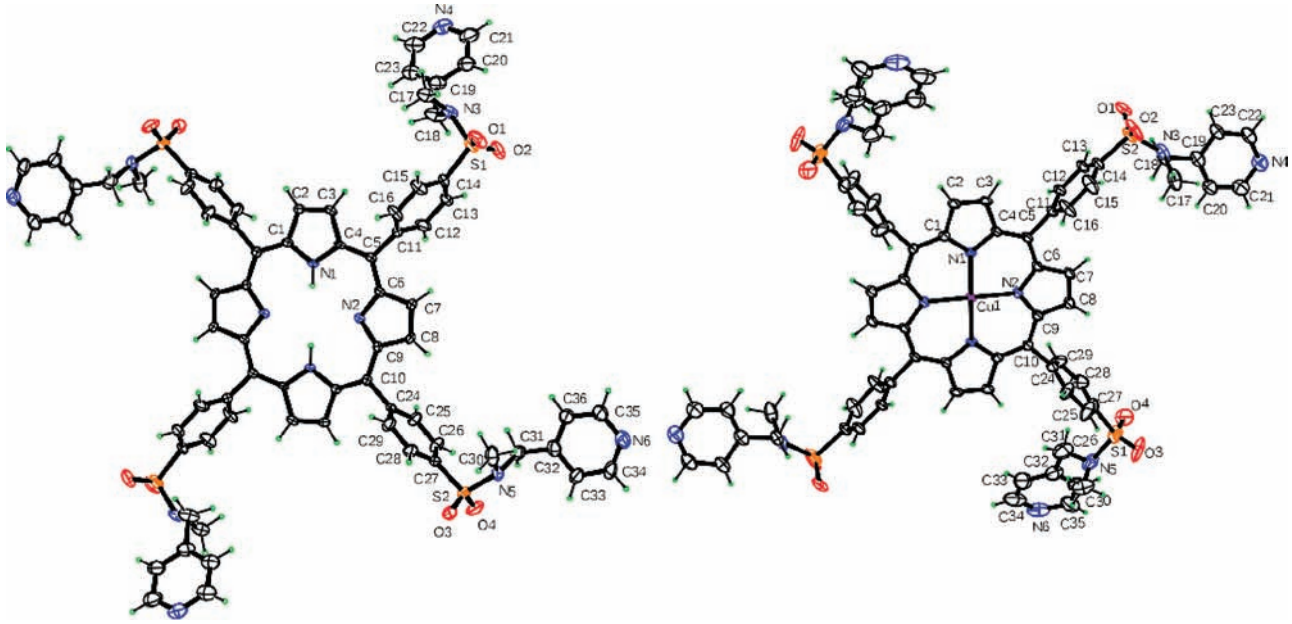

Figure 1. ORTEP drawings of T(*N*-py-4-$CH_2(CH_3)NSO_2Ar$)P (**5**) and Cu(II)**5** with 50% ellipsoids.

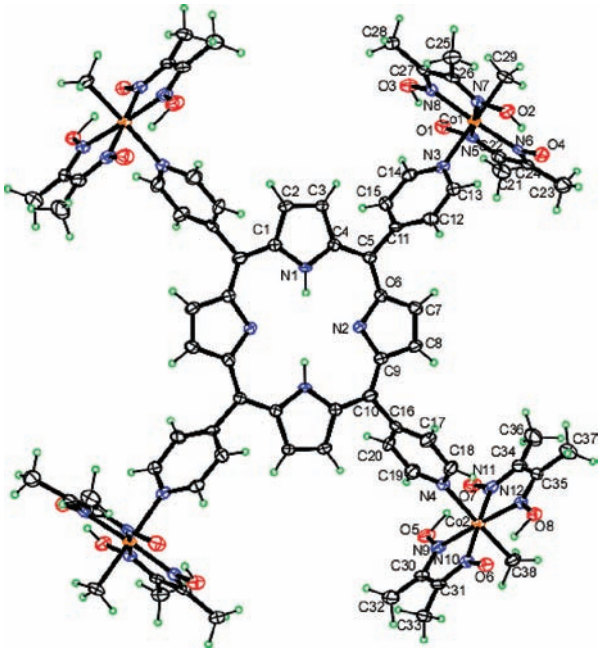

Figure 2. ORTEP drawing of $[CH_3Co(DH)_2]_4$TpyP(4) (**7**) with 50% ellipsoids.

or by insertion of the metal ion into the isolated $[CH_3Co(DH)_2]_4$L adducts. Both methods were efficient and afforded the corresponding zinc and copper complexes in good yield. Because TpyP(4) is not very soluble in chloroform or dichloromethane and the adduct is soluble, metal insertion into the $[CH_3Co(DH)_2]_4$TpyP(4) adduct (**7**) is the preferred method. Insertion of Zn(II) into ($[CH_3Co(DH)_2]_4$T(*N*-py-4-$CH_2(CH_3)NSO_2Ar$)P) (**6**) and **7** led to two Q bands instead of four and a 2 nm red shift of the Soret band, while insertion of Cu(II) led to one Q-band and a 4 nm blue shift of the Soret band; these changes are similar to those found upon metalation of other porphyrins by these metals.[45]

Solution Studies. Porphyrins were characterized by ^{1}H NMR spectroscopy in $CDCl_3$ (Table 3) and DMSO-d_6 (see Experimental Section). The H2,6 signal of $[CH_3Co(DH)_2]_4$T(*N*-py-4-$CH_2(CH_3)NSO_2Ar$)P (**6**) in $CDCl_3$ is slightly upfield to that of T(*N*-py-4-$CH_2(CH_3)NSO_2Ar$)P (**5**) (Table 3 and Figure 3). Coordination of a metal would normally cause downfield shifts of such signals.[5] The upfield shift of H2,6 arises from the anisotropic shielding by Co,[28,29] which more than counteracts the deshielding typically resulting from the inductive effect of a metal. The sharp singlet for the equatorial DH methyls and the broad signal of the oxime O−H−O bridge of the $CH_3Co(DH)_2$ moieties for **6** have shifts of 2.15 ppm and 18.34 ppm, respectively. These shifts are similar to the 2.13 ppm and 18.32 ppm values observed for $CH_3Co(DH)_2$py,[28] as expected. Insertion of Cu(II) and Zn(II) into porphyrin **6** resulted in a general slight upfield shift for the axial methyl signal (Table 3). The H3,5 and H2,6 ^{1}H NMR signals of TpyP(4) and $[CH_3Co(DH)_2]_4$TpyP(4) (**7**) (shown in $CDCl_3$ in Figure 4) are respectively ~0.7 and 0.35 downfield from those of **5** and **6**. Such downfield shifts for TpyP(4) and **7**, as well as the greater downfield shift of H3,5 versus H2,6, could be explained either by an inductive or by an anisotropic effect of the porphyrin core.

When compared to the shifts of the parent TpyP(4), several signals of **7** (Table 3) are moderately or slightly upfield (e.g., the pyridyl H2,6 signal by 0.03 ppm). The upfield shifts of the pyridyl signals arise from the anisotropy of Co.[28,29] In contrast, coordination of four *cis*,*cis*,*cis*-$RuCl_2$(dimethylsulfoxide)$_2$CO units to TpyP(4) caused downfield shifts (H2,6 by 0.45 ppm).[5]

Sharp singlets observed at 2.33 ppm and at 1.03 ppm for the equatorial and axial methyl protons of $[CH_3Co(DH)_2]_4$TpyP(4) (**7**) are shifted downfield by 0.20 ppm when compared to the corresponding signals for $CH_3Co(DH)_2$py.[28] Normally, the axial methyl signal of

(45) Akins, D. L.; Zhu, H. R.; Guo, C. *J. Phys. Chem.* **1996**, *100*, 5420–5425.

Table 3. Selected ^{1}H NMR Shifts (ppm) of Porphyrin and $[CH_3Co(DH)_2]_4$−Porphyrin Signals[a]

compound	O−H···O	Hβ[b]	H3,5 (py)	H2,6 (py)	DH CH_3	Co−CH_3	−NH
T(*N*-py-4-$CH_2(CH_3)NSO_2$Ar)P (**5**)		8.87	7.42	8.70			−2.79
$[CH_3Co(DH)_2]_4$Por**5** (**6**)	18.34	8.85	7.44	8.67	2.15	0.82	−2.79
Cu(II)**6**	18.30		7.38	8.62	2.14	0.80	
Zn(II)**6**	18.18	8.94	7.41	8.63	2.12	0.77	
TpyP(4)		8.87	8.16	9.06			−2.92
$[CH_3Co(DH)_2]_4$TpyP(4) (**7**)	18.53	8.75	8.15	9.03	2.33	1.03	−3.04
Cu(II)**7**	18.23			8.79	2.26	0.96	
Zn(II)**7**	18.42	8.82	8.13	8.97	2.29	0.98	
py			7.29	8.61			
$CH_3Co(DH)_2$py	18.32		7.33	8.61	2.13	0.83	

[a] 5 mM in $CDCl_3$. [b] β -pyrrole.

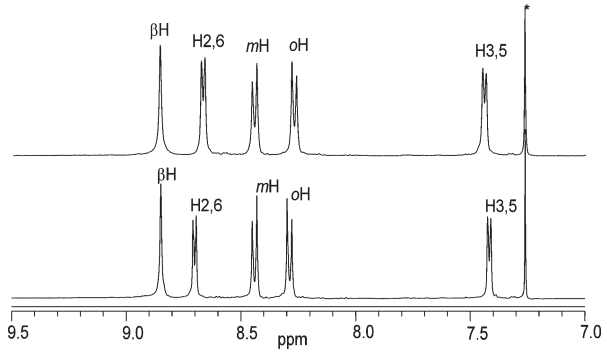

Figure 3. Comparison of the ^{1}H NMR spectra of T(*N*-py-4-$CH_2(CH_3)$-NSO_2Ar)P (**5**) (bottom) and $[CH_3Co(DH)_2]_4$T(*N*-py-4-$CH_2(CH_3)$-NSO_2Ar)P (**6**) (top) in $CDCl_3$.

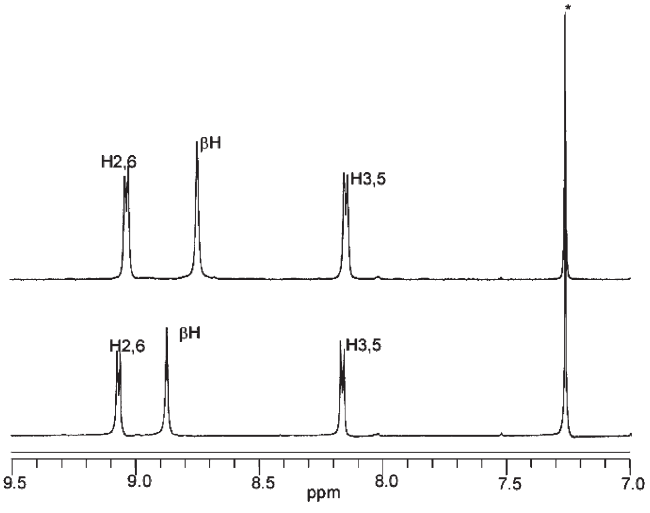

Figure 4. Comparison of the ^{1}H NMR spectra of TpyP(4) (bottom) and $[CH_3Co(DH)_2]_4$TpyP(4) (**7**) (top) in $CDCl_3$.

$CH_3Co(DH)_2$L shifts upfield with increasing L basicity (Supporting Information, Table S2);[29] thus, the downfield shift of the axial methyl observed with L = TpyP(4) indicates either that TpyP(4) peripheral pyridyls are much less basic than pyridine or that the signal is shifted by porphyrin anisotropy. Unlike the axial methyl signal, the equatorial methyl signal of $CH_3Co(DH)_2$L compounds is insensitive to L basicity and tends not to vary much from compound to compound unless L is anisotropic.[26] The usual value is 2.13 ppm (Supporting Information, Table S2); the much further downfield signal for $[CH_3Co(DH)_2]_4$TpyP(4) (**7**) (Table 3) indicates that anisotropy, not basicity, is responsible. Insertion of a metal into **7** to form the Cu(II)**7** and Zn(II)**7** derivatives resulted in a general upfield shift of the signals of the $CH_3Co(DH)_2$ and pyridyl moieties (Table 3). Previous studies have shown that insertion of Zn(II) into TpyP(4) increases the basicity of the pyridyl nitrogen.[46−48] This increased basicity is confirmed by the more upfield shift of the axial methyl signal of Zn(II)**7** compared to **7**. Nevertheless, the downfield shift position of the axial methyl signal of **7**, Cu(II)**7**, and Zn(II)**7** indicates either low pyridyl basicity or a porphyrin anisotropic effect extending out to this long distance. More basic ligands form more stable $CH_3Co(DH)_2$L compounds, and thus we assessed relative binding ability.

A $CDCl_3$ solution initially 10 mM in 3,5-lut and 5 mM in $[CH_3Co(DH)_2]_4$TpyP(4) (**7**) gave a ^{1}H NMR spectrum with signals for $CH_3Co(DH)_2$(3,5-lut), indicating some displacement of the $CH_3Co(DH)_2$ moiety from **7**. The NH signals were most informative. In addition to the NH signal for **7** at −3.04 ppm, NH signals for new species were observed at −3.01, −2.97, −2.94, and −2.92 ppm (Figure 5). In a similar study performed with 40 mM 3,5-lut, the relative size of the NH signals changed. This change and the relative shift trend (the NH signal shifted downfield as the number of $CH_3Co(DH)_2$ moieties displaced increased) allowed assignment of the NH signal to the different adducts. The distribution of the TpyP(4) adducts differing in the number of $CH_3Co(DH)_2$ moieties is summarized in Supporting Information, Table S3.

The $CDCl_3$ solution initially 40 mM in 3,5-lut and 5 mM in $[CH_3Co(DH)_2]_4$TpyP(4) (**7**) revealed considerable displacement of the porphyrin ligand, with 49% of the porphyrin completely lacking a $CH_3Co(DH)_2$ moiety (Supporting Information, Table S3). Two DH methyl peaks were observed. One peak is for $CH_3Co(DH)_2$-(3,5-lut) (2.13 ppm), a value similar to that observed previously.[28,29] The second peak (2.33 ppm) is broad and arises from overlapping signals of $[CH_3Co(DH)_2]_n$TpyP(4) adducts (n = 1, 2, 3 and 4). In solutions of **7** containing 3,5-lut, two signals were observed for the axial methyls. The signal at 0.77 ppm matches that of

(46) Drain, C. M.; Batteas, J. D.; Flynn, G. W.; Milic, T.; Chi, N.; Yablon, D. G.; Sommers, H. *Proc. Natl. Acad. Sci. U.S.A.* **2002**, *99*, 6498–6502.
(47) Drain, C. M.; Nifiatis, F.; Vasenko, A.; Batteas, J. D. *Angew. Chem., Int. Ed. Engl.* **1998**, *37*, 2344–2347.
(48) Drain, C. M.; Nifiatis, F.; Vasenko, A.; Batteas, J. D. *Angew. Chem.* **1998**, *110*, 2478–2481.

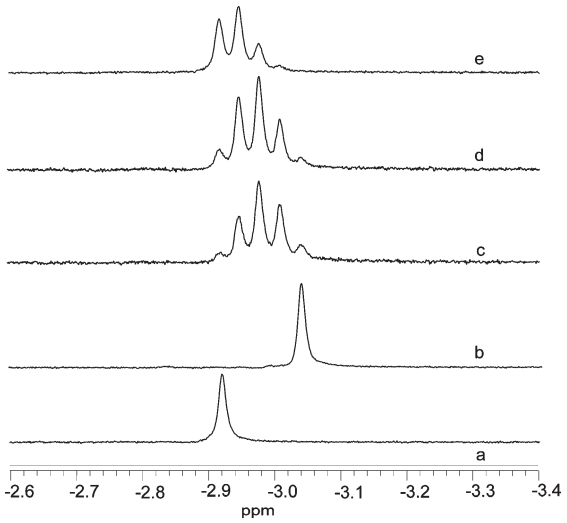

Figure 5. NH ^{1}H NMR signals in $CDCl_3$ of TpyP(4) (a); $[CH_3Co(DH)_2]_4$TpyP(4) (b); $[CH_3Co(DH)_2]_4$TpyP(4): 3,5-lut = 1:2 (c); $[CH_3Co(DH)_2]_4$TpyP(4): 3,5-lut = 1:4 (d); $[CH_3Co(DH)_2]_4$TpyP(4): 3,5-lut = 1:8 (e).

Table 4. Distribution[a] (%) of the $CH_3Co(DH)_2$ Moieties Bound to a Pyridine or Porphyrin on Addition of Pyridines to $CDCl_3$ Solutions of $[CH_3Co(DH)_2]_4$TpyP (4) (**7**) or $[CH_3Co(DH)_2]_4$T(*N*-py-4-$CH_2(CH_3)NSO_2Ar$)P (**6**)

ratio	% of cobalt bound to pyridine	% of cobalt bound to porphyrin
7: 4-CNPy (1:2)	28	72
7: 4-CNPy (1:8)	48	52
7: 3,5-lut (1:2)	51	49
7: 3,5-lut (1:8)	79	21
6: 4-CNPy (1:2)	25	75
6: 4-CNPy (1:8)	40	60
6: 3,5-lut (1:2)	42	58
6: 3,5-lut (1:8)	77	23

[a] Distribution determined from integration of axial CH_3 signals.

$CH_3Co(DH)_2$(3,5-lut), while the other signal (1.03 ppm) is broad and matches that of the $[CH_3Co(DH)_2]_n$TpyP(4) adducts (where n = 1, 2, 3, and 4). By integration of the axial methyl signals, the percentage of $CH_3Co(DH)_2$ moiety bound in TpyP(4) adducts and the percentage in $CH_3Co(DH)_2$(3,5-lut) could be determined (Table 4). In the experiment with 10 mM 3,5-lut (**7**/3,5-lut = 1:2), 51% of the $CH_3Co(DH)_2$ was bound to 3,5-lut, while 49% was still bound to the porphyrin (Table 4); however, in the presence of 40 mM 3,5-lut (**7**/3,5-lut = 1:8), these values were 79% and 21%, respectively (Table 4). A related study was carried out with 4-CNpy and **7** (Table 4 and Supporting Information, Table S3).

The pyridyl group is not directly linked to the porphyrin in $[CH_3Co(DH)_2]_4$T(*N*-py-4-$CH_2(CH_3)NSO_2Ar$)P (**6**); consequently, the NH signal of **6** is not shifted relative to that of **5**. Also, the aromatic signals overlap. Hence, the distribution of the various $[CH_3Co(DH)_2]_n$Por**5** adducts after addition of pyridine ligands could not be assessed. From the relative intensity of the axial methyl signal, the percent distribution of the $CH_3Co(DH)_2$ moiety between the porphyrin adduct and the $CH_3Co(DH)_2$(pyridine ligand) complex could be determined, and the results are summarized in Table 4. The distribution of the $CH_3Co(DH)_2$ moiety between the $CH_3Co(DH)_2$(pyridine ligand) complex and the $[CH_3Co(DH)_2]_n$Por adducts is very similar for Por = T(*N*-py-4-$CH_2(CH_3)NSO_2Ar$)P (**5**) or TpyP(4). Thus, these two porphyrins have similar basicity.

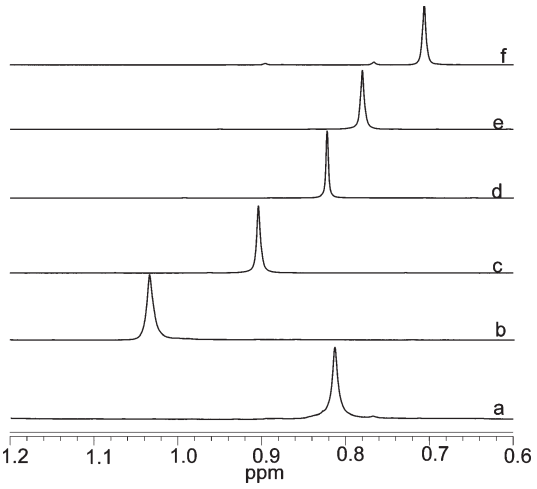

Figure 6. Co-CH_3 region of the ^{1}H NMR spectra of $CH_3Co(DH)_2$L with L = T(*N*-py-4-$CH_2(CH_3)NSO_2Ar$)P (**5**) (a); TpyP(4) (b); 4-CNpy (c); py (d); 3,5-lut (e); and 4-Me_2Npy (f) in $CDCl_3$.

As mentioned, the axial methyl signal shifts of $CH_3Co(DH)_2$(pyridine ligand)[28] are upfield with increasing basicity of the pyridine ligand (Supporting Information, Table S2). The shifts when L = **5**, TpyP(4), 4-CNpy, 3,5-lut, and 4-Me_2Npy are shown in Figure 6, Table 3, and Supporting Information, Table S2. When L = **5**, the axial methyl shift at 0.82 ppm matches that of $CH_3Co(DH)_2$py. These results suggest that the basicity of the pyridyl groups of **5** is close to that of pyridine. The similarity of the adduct distribution in Table 4 thus confirms that TpyP(4) has a basicity comparable to that of **5**. Without doubt the porphyrin ring anisotropy, not low porphyrin basicity, is responsible for the downfield position of the methyl signals in $[CH_3Co(DH)_2]_n$TpyP(4) (**7**).

Visible Absorption Spectra. Soret and Q bands for **5** and TpyP(4) and their respective methylcobaloxime adducts (**6** and **7**) were measured in CH_2Cl_2 (Table 1). The Q and Soret bands correspond respectively to the first and second excited singlet states of the porphyrins.[49−51] The change in the number of Q bands to two or one observed upon insertion of metals (zinc and copper) into the porphyrin results from the increased molecular symmetry (C_{4v} and D_{4h}, respectively), and is typical of patterns observed for metalloporphyrins with the respective metals.[49] The lower symmetry of the Zn porphyrin is attributable to one axial ligand, and X-ray results (albeit of crystals with less than desirable quality) confirmed that an axial water is coordinated in $[CH_3Co(DH)_2]_4$Zn(II) TpyP(4) (Supporting Information, Figure S2).

Compared to the bands of the parent porphyrin (TpyP-(4)), the Soret and Q bands of **7** show 6 nm and ~4 nm red shifts, respectively (Table 1). The spectrum of **6** retains the

(49) Spellane, P. J.; Gouterman, M.; Antipas, A.; Kim, S.; Liu, Y. C. *Inorg. Chem.* **1980**, *19*, 386–391.
(50) *The Porphyrins:* Dolphin, D., Ed.; Academic Press: New York, 1978; Vol. 3.
(51) Even, U.; Magen, J.; Jortner, J.; Friedman, J.; Levanon, H. *J. Chem. Phys.* **1982**, *77*, 4374–4383.

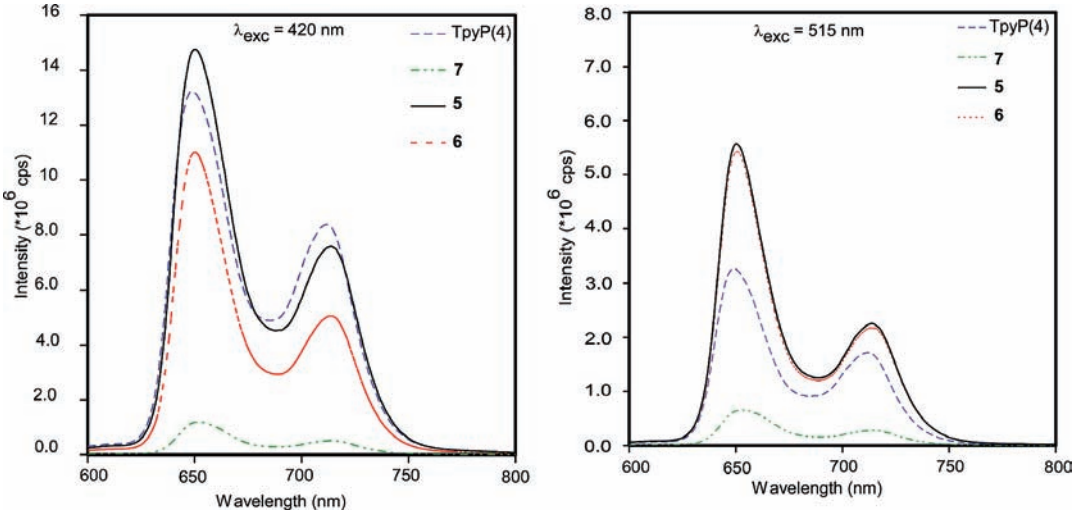

Figure 7. Emission spectra in CH_2Cl_2 of T(*N*-py-4-$CH_2(CH_3)NSO_2Ar$)P (**5**), $[CH_3Co(DH)_2]_4$T(*N*-py-4-$CH_2(CH_3)NSO_2Ar$)P (**6**), TpyP(4), and $[CH_3Co(DH)_2]_4$TpyP(4) (**7**) at excitation wavelengths of 420 nm (left) and 515 nm (right).

characteristic Soret and Q bands of the parent porphyrin **5**, with no shifts (Table 1). The red shift of the Soret band observed with the $[CH_3Co(DH)_2]_4$TpyP(4) adduct (**7**) (Table 1) suggests that there is a reduction of the electron density as a result of cobalt coordination to the pyridyl groups. In contrast, the lack of a shift for the $[CH_3Co(DH)_2]_4$T(*N*-py-4-$CH_2(CH_3)NSO_2Ar$)P adduct (**6**) is expected because the pyridyl groups are not directly linked to the porphyrin core. The blue shift (4 nm) of the Soret band and of one Q-band (540 nm) observed for copper complexes Cu(II)**6** and Cu(II)**7** (Table 1) is consistent with observations reported for other copper porphyrins.[52,53] In copper porphyrins the delocalized π bonding decreases the average electron density, which increases the energy needed for electronic transitions, and thus a blue shift of the Soret band is observed.[54] Complexes Zn(II)**6** and Zn(II)**7** show a red shift (< 10 nm) of the Soret band and two Q bands (550, 596 nm), as observed previously with other zinc porphyrins.[53] For zinc porphyrins the delocalized π bonding increases the average electron density of the porphyrin, thus lowering the energy for the electronic transition and leading to a red shift of the Soret band.[54]

Emission Spectra. The emission of T(*N*-py-4-$CH_2(CH_3)NSO_2Ar$)P (**5**) and of TpyP(4) in dichloromethane is compared to that of the $CH_3Co(DH)_2$ adducts (Table 1). The fluorescence intensity of **5** is comparable to that of TpyP(4) upon selective excitation at the Soret band (420 nm; Figure 7). The adducts, $[CH_3Co(DH)_2]_4$T(*N*-py-4-$CH_2(CH_3)NSO_2Ar$)P (**6**) and $[CH_3Co(DH)_2]_4$TpyP(4) (**7**), show typical porphyrin-based intense fluorescence spectra (Figure 7) characterized by two bands at ~650 and ~714 nm (λ_{exc} = 420 or 515 nm).[45] A small red shift (~3 nm) of the emission bands of **7** was observed with respect to the parent porphyrin (TpyP(4)). Insertion of zinc (Zn(II)**6** and Zn(II)**7**) changed the general shape of the emission spectra and led to a blue shift (50 nm, λ_{exc} = 420 nm) of the emission bands (~600 and 650 nm) (Table 1) compared to those of the metal-free porphyrins (**6** and **7**). The intensity of spectra obtained on optically matched (λ_{exc} = 420 nm) solutions showed that the emission of **6** is slightly lower (25−35%) for both bands (650 and 714 nm) than that of **5**. The fluorescence intensity of **7** (λ_{exc} = 420 nm) is generally much lower (90%, for both the 652 and 714 nm bands) than that of TpyP(4) (Figure 7). The much greater effect of adduct formation on **7** than on **6** is attributable to the direct and indirect attachment of the pyridyl group to TpyP(4) and T(*N*-py-4-$CH_2(CH_3)NSO_2Ar$)P, respectively, resulting from a much shorter distance of the methylcobaloxime moieties to the porphyrin in **7** than in **6**. The quenching of the emission of **7** is attributed to the cobalt heavy atom effect. Heavy atoms enhance spin−orbit coupling of a formally spin-forbidden deactivation process of the singlet state of the porphyrin.[11]

The titrations of 4-CNpy, 3,5-lut, and 4-Me_2Npy into 5 μM solutions of adducts **6** and **7** in dichloromethane were monitored by fluorescence spectroscopy; results for 4-CNpy and 4-Me_2Npy are shown for **6** and **7** in Figure 8 and Supporting Information, Figures S3 and S4. When a solution of **7** was titrated with these pyridine ligands, fluorescence intensity restoration was observed. Upon addition of 4-Me_2Npy (80 μM) (Figure 8), the restored fluorescence intensity at 650 nm was 12 times that of the original solution of **7**; the values obtained with 3,5-lut and 4-CNpy (80 μM) (Supporting Information, Figure S4) were 11 and 5 times the original fluorescence, respectively. The titration of TpyP(4) with 4-Me_2Npy resulted in an intensity ~1.2 times that of the original value of TpyP(4). These results support the conclusion that restoration of fluorescence intensity upon addition of the different pyridine ligands is caused by the displacement of the $CH_3Co(DH)_2$ moieties, releasing the TpyP(4).

The fluorescence intensity of **6** increased by ~1.5 times upon the addition of 4-CNpy (Supporting Information, Figure S3), 3,5-lut, or 4-Me_2Npy (Figure 8) (80 μM). The titration of **5** with 4-Me_2Npy led to a ~1.2 times increase of the original fluorescence intensity. This higher intensity is similar to that observed upon titrating **6** with the different pyridine derivatives; as a result, we conclude

(52) Butje, K.; Nakamoto, K. *Inorg. Chim. Acta* **1990**, *167*, 97–108.
(53) Sun, X.; Chen, G.; Zhang, J. *Dyes Pigm.* **2008**, *76*, 499–501.
(54) Zheng, W.; Shan, N.; Yu, L.; Wang, X. *Dyes Pigm.* **2008**, *77*, 153–157.

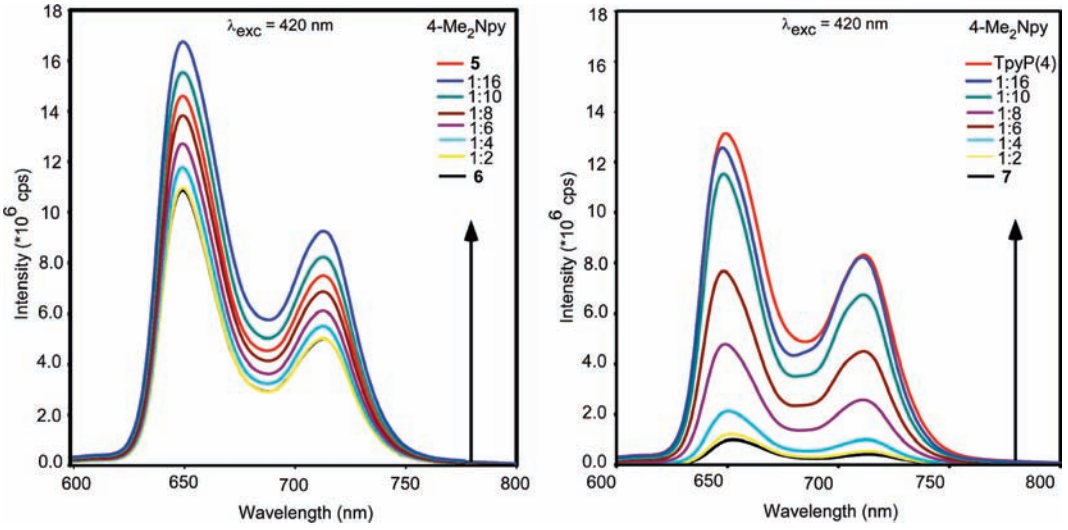

Figure 8. Emission spectra of $[CH_3Co(DH)_2]_4T(N\text{-py-4-}CH_2(CH_3)NSO_2Ar)P$ (**6**) (left) and $[CH_3Co(DH)_2]_4TpyP(4)$ (**7**) (right) (5.0 μM) in CH_2Cl_2 with increasing amounts (6/7: pyridine ratio) of 4-Me_2Npy.

that the increase in fluorescence intensity of solutions of **6** arises from a combination of two effects of the pyridine ligands: first, displacement of the $CH_3Co(DH)_2$ moieties and second, weak interaction with the displaced porphyrin.

Conclusions

The synthetic scheme developed in this work is useful and versatile for preparing porphyrins and metalloporphyrins having sulfonamides and peripheral pyridyls. However, it is necessary to employ a tertiary sulfonamide because otherwise intractable species are formed. Adducts with four methylcobaloxime units bound to pyridylporphyrins (TpyP(4) and T(*N*-py-4-$CH_2(CH_3)NSO_2Ar$)P) have been synthesized, and their photophysical properties investigated and compared to those of the parent porphyrin. Upon excitation of the porphyrin core, the typical porphyrin fluorescence is partially quenched for the $[CH_3Co(DH)_2]_4T(N\text{-py-4-}CH_2(CH_3)NSO_2Ar)P$ adduct (**6**), whereas the fluorescence of the $[CH_3Co(DH)_2]_4TpyP(4)$ adduct (**7**) is strongly quenched. These observations suggest that the porphyrin core of T(*N*-py-4-$CH_2(CH_3)NSO_2Ar$)P is insulated from the pyridyl group, and consequently coordination of the methylcobaloxime moiety to the pyridyl group does not greatly modulate the photophysical properties of the porphyrin. A comparison of the ^{1}H NMR signal of the axial methyl of the T(*N*-py-4-$CH_2(CH_3)NSO_2Ar$)P and the TpyP(4) methylcobaloxime adducts with those of the other methylcobaloxime compounds with different pyridine ligands allows us to conclude that the pyridyl groups of T(*N*-py-4-$CH_2(CH_3)NSO_2Ar$)P) and of TpyP(4) have a basicity (and hence metal-binding ability) close to that of pyridine. In turn, the porphyrins do not affect the properties of the cobaloxime moiety. The unusual downfield shift found for the $CH_3Co(DH)_2$ methyl signals in **7** can be confidently attributed to porphyrin ring anisotropy.

Acknowledgment. We acknowledge the steadfast interest and encouragement for our studies with porphyrins from the late Professor Peter Hambright of Howard University, and we dedicate this paper and the accompanying paper to his memory. We thank Dr. Steven Soper's research group for the use of their fluorimeter. Purchase of the diffractometer was made possible by Grant LEQSF(1999-2000)-ENH-TR-13, administered by the Louisiana Board of Regents.

Supporting Information Available: Tables of selected bond distances and angles of the methylcobaloxime moieties in $[CH_3Co(DH)_2]_4TpyP(4)$ (**7**), NMR data for $CH_3Co(DH)_2$(pyridine) compounds, and distribution of species upon addition of pyridines to $[CH_3Co(DH)_2]_4$(porphyrin) compounds; ^{1}H NMR spectra of all the new compounds; emission spectra for T(*N*-py-4-$CH_2(CH_3)NSO_2Ar$)P (**5**) and **7** in CH_2Cl_2 with increasing amounts of added 4-CNpy; ORTEP drawings of T(*N*-py-2-$CH_2(CH_3)NSO_2Ar$)P (**4**) and $[CH_3Co(DH)_2]_4Zn(II)TpyP(4)$ **(Zn(II)7)**; crystallographic data of T(*N*-py-2-$CH_2(CH_3)NSO_2Ar$)P (**4**), T(*N*-py-4-$CH_2(CH_3)NSO_2Ar$)P (**5**), Cu(II)**5** and $[CH_3Co(DH)_2]_4TpyP(4)$ (**7**) in CIF format. This material is available free of charge via the Internet at http://pubs.acs.org.